Numerical Modeling of Berm Breakwater Optimization with Varying Berm Geometry Using REEF3D

Athul Sasikumar*[1], Arun Kamath[2], Onno Musch[1], Hans Bihs[2], and Øivind A. Arntsen[2]

[1]Coastal Engineering, Norconsult AS, Klæbuveien, Trondheim, 7031, Norway
[2]Department of Civil and Environmental Engineering, Norwegian University of Science and Technology (NTNU), 7491 Trondheim, Norway

Journal of Offshore Mechanics and Arctic Engineering, 2019, **141** , pp. 011801-1-10.
DOI: http://dx.doi.org/10.1115/1.4040508

Abstract

Harbours are important infrastructures for an offshore production chain. These harbours are protected from the actions of sea by breakwaters to ensure safe loading, unloading of vessels and also to protect the infrastructure. In current literature, research regarding the design of these structures is majorly based on physical model tests. In this study a new tool, a three-dimensional numerical model is introduced. The open-source CFD (Computational Fluid Dynamics) model REEF3D is used to study the design of berm breakwaters. The model uses the Volume averaged Reynolds Averaged Navier-Stokes (VRANS) equations to solve the porous flows. At first the VRANS approach in REEF3D is validated for flow through porous media. A dam break case is simulated and comparisons are made for the free surface both inside and outside the porous medium. The numerical model REEF3D is applied to show how to extend the database obtained with purely numerical results, simulating different structural alternatives for the berm in a berm breakwater. Different simulations are conducted with varying berm geometry. The influence of the berm geometry on the pore pressure and velocities are studied. The resulting optimal berm geometry is compared to the geometry according to empirical formulations.

Keywords: breakwater; berm; REEF3D; coastal structures; Computational Fluid Dynamics;

*Corresponding author,athul.sasikumar@norconsult.com
Postprint, published in Journal of Offshore Mechanics and Arctic Engineering, doi:http://dx.doi.org/10.1115/1.4040508

1 Introduction

The design of coastal structures has been increasingly difficult due to the growing scale of projects and multitude of functions competing for vital space in coastal areas. This has resulted in the need for optimum solutions in coastal engineering projects, especially the design of coastal structures. A breakwater is a common example for such coastal structures which are built to protect a coast or harbour from wave action. The focus of the current study is on the berm breakwaters which can be either dynamically or statically stable (Fig. 1a). A berm breakwater is a rubble mound breakwater with a berm on the seaward side. The behaviour of the berm is an important aspect in the design of berm breakwaters and can be described as: hardly reshaping, partly reshaping or fully reshaping. An important measure for the reshaping is the recession (Rec) of the berm and is defined as shown in Fig. 1b.

The design of berm breakwaters has been traditionally based on two basic tools: semi-empirical formulations and physical models. They both allow the designer to include the operability, functionality and reliability requirements. The advantages of semi empirical formulations CIRIA et al. CECW-EH are that they are fast and inexpensive. However, these formulations are not strictly applicable outside the conditions that they were derived for and are not applicable for structures with non-conventional sections or with important local effects. The scaled physical modelling in a laboratory is one of the key methods in the design of berm breakwaters. The advantage of physical models is that it reduces the uncertainty when obtaining the structural response and is specially necessary when the structures are non-conventional or when three-dimensional effects are present. Nevertheless, this approach presents certain limitations: intrusive measuring devices, scale effects and high cost (in time and money) of the experiments.

This study introduces an alternative tool in the design process of berm breakwaters: numerical modelling. In order to obtain accurate numerical results, the model must be validated to prove that it is capable of reproducing the processes of interest. Moreover, if the model depends on calibration parameters, they need to be correctly adjusted. In either case, this is to be performed by comparing the model results with experimental results. The use of numerical modelling for the design of berm breakwaters must be regarded as a complementary tool to physical modelling. A numerical model for the design of berm breakwaters can be used for two main roles,

1. Assisting with the pre-design of the physical experiments.

2. Extending the experimental database with detailed results, after validation.

The focus of this study is to test the use of the numerical model REEF3D for the design of berm breakwaters. REEF3D has been succesfully used for a range of marine applications, such as breaking wave forces Kamath et al. (2016), floating body dynamics Bihs and Kamath (2016) or sloshing Grotle et al. (2016). The stability of berm breakwaters are influenced by many variables such as the wave, structural and material characteristics. This paper will focus on the structural characteristics of the berm: berm slope, berm width and the berm height influence on the wave kinematics inside the core of the berm breakwater. In this study, volume averaging of Navier-Stokes equations (VRANS) is used to solve the porous media flow which considers the porous medium as a continuous media and thereby eliminating the need for a detailed resolution of the individual rock components. The VRANS method yields very

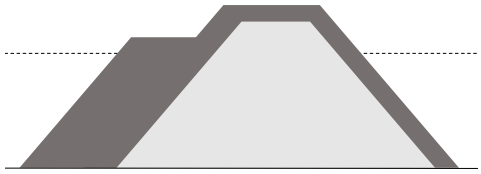

(a) Dynamically/statically stable berm breakwater

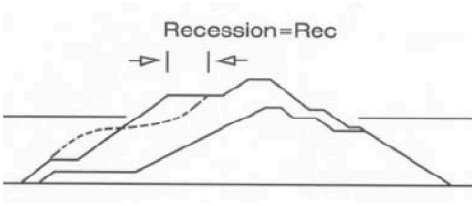

(b) Recession of berm breakwaters van der Meer and Sigurdarson (2013)

Figure 1: Berm breakwaters and R*ec* parameter

detailed solution including the pressure and velocity fields both outside and inside the porous medium based on volume averaging of the RANS equations. The effects of turbulence within the porous medium are accounted for with the two equation $k-\omega$ turbulence model and the free surface is obtained using the level set method. The applied type of porosity model relies on empirical resistance coefficients which often need to be measured or calibrated.

The numerical model REEF3D is validated for a 2D dam break case based on the experiments carried out by Liu et al. Liu et al. (1999). Once the validation is completed and the predictive capabilities of REEF3D is assured, berm breakwaters are introduced. The influence of berm height, berm width and berm slope on the pore pressure and the velocities is investigated. The use of numerical modelling to extend the database of the changes in wave kinematics with different structural alternatives will be studied.The optimal berm geometry based on the lowest values of pore pressure and velocities are compared with the berm geometry according to empirical relations.

Numerical Model

Governing equations

The numerical model REEF3D uses the three-dimensional Reynolds-Averaged Navier-Stokes equation (RANS) to describe the incompressible fluid flow. These RANS equations are solved together with the continuity equation for prescribing momentum and mass conservation:

$$\frac{\partial u_i}{\partial x_i} = 0 \tag{1}$$

$$\frac{\partial u_i}{\partial t} + u_j \frac{\partial u_i}{\partial x_j} = -\frac{1}{\rho}\frac{\partial p}{\partial x_i} + \frac{\partial}{\partial x_j}\left[(\nu + \nu_t)\left(\frac{\partial u_i}{\partial x_j} + \frac{\partial u_j}{\partial x_i}\right)\right] + g_i \tag{2}$$

In Eq. 1 and 2, u is the velocity averaged over time t, p is the pressure, ρ is the fluid density, ν is the kinematic viscosity, ν_t is the eddy viscosity and g the acceleration due to gravity. The pressure is determined using Chorin's projection method Chorin (1968) and HYPRE solver Center for Applied Scientific Computing (2006) is used to solve the resulting Poisson pressure equation. The eddy viscosity ν_t in the RANS equations is determined using the two-equation k-ω model Wilcox (1994). The convective terms of the RANS equations are discretized with the fifth-order WENO scheme Jiang and Shu (1996) in the conservative finite-difference framework. REEF3D uses a Cartesian grid for spatial discretization and a

ghost cell immersed boundary method (GCIBM) Berthelsen and Faltinsen (2008) is used to account for the complex geometric solid-fluid boundaries. The code is fully parallelised using the MPI library and the numerical model can be executed on high performance computing systems with very good scaling.

Numerical Wave Tank

The present numerical model is used as a numerical wave tank Bihs et al. (2016). The numerical wave tanks is based on RANS equations with the free surface description through the level set method. In order to replicate the behaviour of a physical wave tank the boundary conditions of the numerical wave tank need to be chosen to recreate physical behaviour. The numerical wave tank consists of 6 boundaries: inlet, outlet, atmosphere, bottom and front and back.

The numerical model REEF3D provides different methods for wave generation and absorption. For example, relaxation method Jacobsen et al. (2012) can be used for both wave generation and absorption. In this method, the analytical solution form wave theory is used to moderate the computationally generated waves in the wave tank. The computational values of velocity and free surface are taken from zero to the analytical values expected by wave theory in the wave generation zone. Similarly, at the numerical beach the computational value of velocity and free surface are brought to zero and all the energy is smoothly removed from the wave tank. Here the wave generation occurs in a relaxation zone with size typically of one wavelength (Fig. 2). The values for velocity and free surface are moderated in the relaxation zones for wave generation and absorption using the following equation:

$$\begin{aligned} u_{relaxed} &= \Gamma(x) u_{analytical} + (1 - \Gamma(x)) u_{computational} \\ \phi_{relaxed} &= \Gamma(x) \phi_{analytical} + (1 - \Gamma(x)) \phi_{computational} \end{aligned} \tag{3}$$

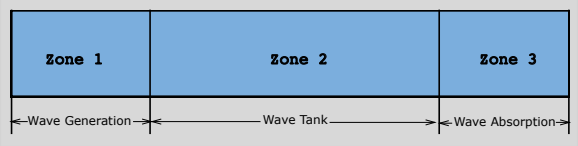

Figure 2: Sections of a Numerical Wave Tank

Level set method

In order to model the free surface, the level set method given by Osher and Sethian(1988) Osher and Sethian (1988) is used since it enables to obtain complex changes. In this method, the zero level set of a signed distance function, $\phi\left(\overrightarrow{x}, t\right)$ called the level set function is used. The level set function provides the distance to the interface Γ and the 2 phases are represented by the change of the sign of the level set function. For the remaining domain, the level set function represents the closest distance of each point in the domain from the interface and the sign distinguishes the two fluids across the interface. The level set function is defined as:

$$\phi(\vec{x},t)\begin{cases} > 0 & if\ \vec{x}\ is\ in\ phase\ 1 \\ = 0 & if\ \vec{x}\ is\ at\ the\ interface \\ < 0 & if\ \vec{x}\ is\ in\ phase\ 2 \end{cases} \tag{4}$$

The level set function is smooth across the interface and provides a sharp description of the free surface. The level set function is convected under the velocity field in the wave tank. The signed distance property of the function is lost by the motion of the free surface and it is restored by reinitialising the function after every iteration using the partial differential equations based on the procedure by Peng et al. Peng et al. (1999).

VRANS

Averaging of the RANS equations to solve flow in a porous medium can be done in several ways. In this study the numerical model uses the Volume-averaged Reynolds-Averaged Navier-Stoke equations (VRANS) and is implemented based on the work presented by Jensen et al. (2014) Jensen et al. (2014). Jensen's work includes the different equations found in literature with details regarding the underlying assumptions and their range of application. A porous medium is shown in Fig. 3, where S is the surface which includes both solid phase and fluid phase which creates the averaging volume and is defined by a radius r. In the volume averaging process, the total volume V remains the same while the actual volume of the fluid phase may vary depending on the position of the volume averaging. The volume averaging process is applied with the length scale constraints given as $l \ll r \ll L$, where l is the pore length scale and L is the macroscopic length scale.

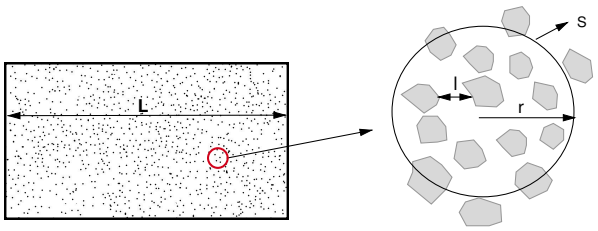

Figure 3: Volume averaging in porous media

The volume averaging process converts the RANS equation to the VRANS equations. The starting point is the incompressible RANS equations formulated with the continuity equation (Eq. 5) and momentum equation (Eq. 6).

$$\frac{\partial u_i}{\partial x_i} = 0 \tag{5}$$

$$\frac{\partial u_i}{\partial t} + u_j\frac{\partial u_i}{\partial x_j} = -\frac{1}{\rho}\frac{\partial p}{\partial x_i} + \frac{\partial}{\partial x_j}\left[(\nu+\nu_t)\left(\frac{\partial u_i}{\partial x_j}+\frac{\partial u_j}{\partial x_i}\right)\right] + g_i \tag{6}$$

Applying the volume averaging theorem Howes and Whitaker (1984) to the continuity equation together with the assumption that the velocities on the solids being zero results in Eq. 7. Here $\langle\bar{u_i}\rangle$ is the velocity averaged over the volume and is called as the filter velocity. The continuity equation mentioned in Eq. 5 is to represent the volume density of the outward

flux of a vector field from an extremely small volume around a pore. The correct representation of the continuity equation is that the divergence of the filter velocity is zero ($\nabla \langle \bar{u} \rangle = 0$). This means that the filter velocity will be constant in the flow direction and when the volume is averaged over the entire volume, it will have zero flux for the velocity field. This will provide a divergence free velocity field when the entire volume is volume averaged in the continuity equation.

$$\frac{\partial \langle \bar{u_i} \rangle}{\partial x_i} = 0 \tag{7}$$

Similarly for the momentum equation (Eq. 6), each term in the equation is volume averaged. The formulations are based on filter velocities which are divided by the porosity to get the correct momentum contributions. The momentum equation for the porous media then becomes:

$$\begin{aligned} (1 + C_m) \frac{\partial}{\partial t} \frac{\bar{u_i}}{n} + \frac{1}{n} \frac{\partial}{\partial x_j} \frac{\bar{u_i} \bar{u_j}}{n} = \\ \rightarrow -\frac{1}{\rho} \frac{\partial \bar{p}^f}{\partial x_j} - g + \frac{1}{n} \frac{\partial}{\partial x_j} \mu \left(\frac{\partial \bar{u_i}}{\partial x_j} + \frac{\partial \bar{u_j}}{\partial x_i} \right) + F_i \end{aligned} \tag{8}$$

$$F_i = -a\rho \langle \overline{u_i} \rangle - b\rho \sqrt{\langle \overline{u_j} \rangle \langle \overline{u_j} \rangle \langle \overline{u_i} \rangle} \tag{9}$$

Here, F_i on the right hand side of Eq. 8 represents the effect of turbulence in terms of additional resistance. This is modelled using the extended Darcy-Forcheimmer equation which includes the linear and non-linear forces and also the inertial forces for local accelerations and is given by Eq. 9. Here a and b are the resistance coefficients and are defined by Eq. 10 and Eq. 11 van Gent (1992b). In the relation for a and b, d_{50} is the grain diameter and KC is the Keulegan-Carpenter number which represent the ratio between the turbulence and inertia effects.

$$a = \alpha \frac{(1-n)^2}{n^3} \frac{v}{\rho d_{50}^2} \tag{10}$$

$$b = \beta (1 + \frac{7.5}{KC}) \frac{(1-n)}{n^3} \frac{1}{d_{50}} \tag{11}$$

The coefficients α and β have to be determined experimentally which depend on the Reynolds number, shape of the stones, permeability and grade of porous material. The existing knowledge on the variation of resistance coefficients originates from theoretical considerations, physical experiments and numerical calibrations. In Eq. 8, C_m is the added mass coefficient which takes the grain-water interaction interaction into account. Van Gent (1992) van Gent (1992a) derived a expression for this and is given in Eq. 12 where n is the porosity and γ_p is empirical coefficient which takes the value 0.34.

$$C_m = \gamma_p \frac{1-n}{n} \tag{12}$$

The use of a filter velocity in the momentum equation will result in different values for pressure gradients both inside and outside the porous media. So, the pressure needs to be

defined as pore pressure in momentum equations so that the hydrostatic pressure distribution both inside and outside the porous medium will be linear and identical. In order to track the free surface inside the porous medium, the level set method is used. The change in interface (Γ) due to the changes in velocity field ($\overrightarrow{u}$), a convection equation for the level set function is obtained in the VRANS framework as shown in Eq. 13.

$$\frac{\partial \phi}{\partial t} + \frac{u_j}{n}\frac{\partial \phi}{\partial x_j} = 0 \tag{13}$$

RESULTS

Validation of Numerical model

The previously defined equations for porous media requires calibration for resistance coefficients. The first validation case is based on the experiments carried out by Liu et al. Liu et al. (1999) for dam break flow.

2D Dam break

Liu et al. Liu et al. (1999) conducted experiments for a dam break flow through a porous medium. The experiments were performed inside a glass tank (89 cm horizontally and 58 cm vertically) along with the use of video recording techniques to obtain the free surface elevation both inside and outside the porous medium.

The general setup of the dam break experiment is given in Fig. 4. The porous dam was kept in the middle of the tank which was 29 cm long and 58 cm high. The water was set to flow from the left side of the tank and is separated from the porous medium using a moving gate. This gate was placed 2 cm from the porous medium and thereby creating a reservoir with a certain depth. At the beginning of the experiments the gate is opened manually within about 0.1 s. Further details about the experiments can be found in Liu et al. Liu et al. (1999). The properties of the porous material used for the experiment are:

1. Glass beads: $D_{n50} = 3.0$ mm, $n = 0.39$

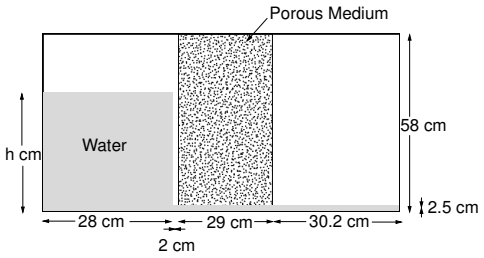

Figure 4: Setup for 2D dam break

Porous medium with Glass beads

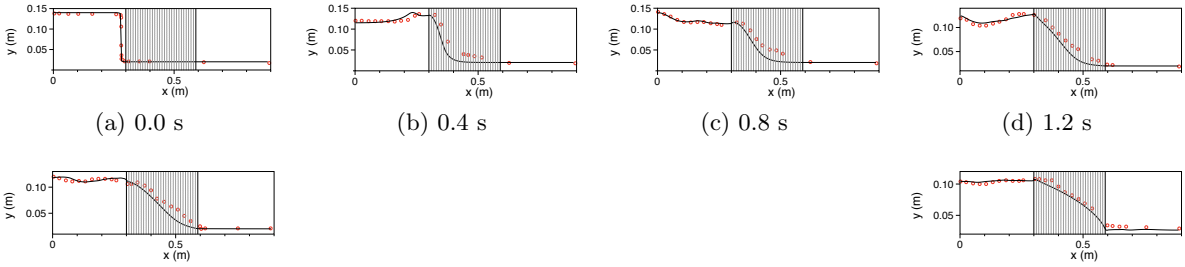

(a) 0.0 s (b) 0.4 s (c) 0.8 s (d) 1.2 s

(e) 1.6 s (f) 4.0 s

Figure 5: Comparison of free surface profiles for flow passing through porous medium - Glass beads. Red dots indicate experimental data and black line indicate numerical data

The experimental tank is reproduced numerically with the porous dam placed at the centre of the domain and a uniform grid resolution is applied throughout the domain with a grid size of dx=0.5 cm. The water level is kept at 14 cm. Liu et al. Liu et al. (1999) reported the Reynolds numbers for the glass bead experiments as roughly 100 which corresponds to a Forchheimer flow regime. The flow regimes defined based on the pore Reynolds number are as follows,

1. R_{ep} <1 = Darcy (Laminar flow regime)
2. 1 <R_{ep} <10 = Inertial flow regime
3. 10 <R_{ep} <150 = The Forchheimer flow regime
4. 150 <R_{ep} <300 = The transitional flow regime
5. R_{ep} >300 = The fully turbulent flow regime

Since the flow regime corresponds to a Forchheimer regime, a strong dependency on the α parameter is expected. A calibration is performed by completing a simulation matrix, where the α coefficient is varied as $\alpha = [25, 50, 75, 100, 200, 300, 500, 650]$ and β is kept as 1.1. The combination of α= 100 and β= 1.1 gives the best agreement. It can be seen in Fig. 5 that the agreement in general is very good with few discrepancies in the agreement. One explanation for the slight disagreement are because during the lab experiments the free surfaces in the porous dam have been found to stick on the glass wall at some locations Liu et al. (1999). This is probably caused because of the surface tension and capillary effect and which may result in overestimating the free surface inside the porous dam.

Berm breakwaters

The focus of the study is on the influence of structural characteristics on the wave kinematics inside a berm breakwater. Two main parameters; pressure and velocity describing the wave kinematics will be analysed with varying berm geometry. The recession of the berm breakwaters cannot be accounted for in the current model and therefore a statically stable berm breakwater is modelled. The different classifications of berm breakwaters according to the PIANC WG40 report PIANC (2003) is shown in Table 1. The main stability parameter

in designing a berm breakwater is the stability number, N_s=H_o=$H_s/(\Delta D_{n50})$ where H_s is the significant wave height, $\Delta = \rho_s/\rho_w$ - 1 where ρ_s and ρ_w are the mass density of rock and water respectively.

Here, D_{n50} (median nominal diameter) is used instead of the D_{50} parameter (median diameter) since it is not possible to sieve these large rocks to derive at a D_{50} value. The median nominal diameter is defined as D_{n50} =$(M_{50}/\rho_s)^(1/3)$ where ρ is the stone density, M_{50} is the median weight of stones. According the ROCK MANUAL CIRIA et al., M_{50} is the mass of the theoretical block for which half of the mass of the sample is lighter.

Apart from the stability number, van der Meer van der Meer (1998) introduced the dimensionless wave height-wave period parameter H_oT_{om}=$H_oT_m(g/D_{n50})^{0.5}$ for berm breakwaters. For a statically stable berm breakwater, the stability number must be in the order of 1.5 to 2 and the dimensionless wave height-wave period parameter between 20 and 40. The stability number for the berm modelled here corresponds to N_s = 1.79 and the dimensionless wave height-wave period parameter H_oT_{om} = 31.71.

Table 1: Classification of berm breakwaters according to PIANC MarCom Report of WG 40.

Type	N_s=H_o	H_oT_{om}
Statically stable, no reshaping of berm, negligible erosion of front	<1.5 - 2	<20 - 40
Statically stable, some reshaping of berm in design sea states	1.5 - 2.7	40 - 70
Dynamically stable, larger reshaping, movement of stones	>2.7	>70

The berm breakwater is represented inside the 2D Numerical Wave Tank (NWT) of REEF3D . The 2D NWT is 10.0 m long and 1.2 m high with the berm breakwater centre being 6.0 m away from the wave generation (Fig. 6). A uniform grid size of 1.0 cm is used in the entire domain which resulted in a total of 1.2 million cells. A wave generation zone is defined at the start of the NWT (X = 0 m to X = 3 m).The boundary conditions have been assigned based on the relaxation method to both generate and absorb the waves. The next zone represents the working zone (X = 3 m to X = 7 m) where the berm breakwater is placed. A wave absorption zone is defined at the end of the NWT (X = 7 m to X = 10 m) in-order to make sure that there is no reflection from the end of the tank and is based on the relaxation method. The type of regular waves generated here are the 5^{th}-order Stokes waves with H_s=0.2 m,T_s=1.5 s and the water depth is set at d=0.7 m. The resistance coefficients are taken from existing literature Troch (2000).

1. Berm: D_{n50} = 0.07 m, n = 0.51, α= 1000 and β= 1.0
2. Core: D_{n50} = 0.03 m, n = 0.39, α= 600 and β= 2.2

Berm height vs. Velocity and Pressure

For berm breakwaters, it is interesting to see how the berm influences the wave kinematics inside the breakwater. Pore velocity is affected by the porosity of the porous media along with turbulence which can play an important role as well. Not only the velocities, but also the

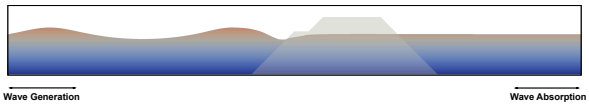

Figure 6: Set up for berm breakwater in Numerical Wave Tank

pressure at different points along the core of the breakwater can give interesting information about the flow that occurs inside the breakwater. First, the influence of berm height is analysed. A berm height parameter was identified as h_B/d , where h_B is the height of the berm and d the water depth. This term accounts for the difference in the ability of the berm breakwaters to dissipate wave energy as the height of the berm increases or decreases. Different simulation are performed with berm height to water depth ratio (h_B/d) varying from 0.07 to 1.43. The berm width is kept at a fixed value of W=0.25 m, a slope of 1:1.25, a water depth of d= 0.7 m and the crest height is set at 1.0 m. A representation of berm geometry with h_B/d ratio of 1.14 is shown in Fig. 7 with locations of probes for both pressure and velocities indicated by red dots. A total of three probes are placed inside the core of the berm breakwater. Two probes are placed right after and before the seaward and leeward face of the core and one is placed at the centre of the core. The measured velocities in these 3 probes with different berm elevation is shown in Fig. 8a, 8b, 8c and the pressure measurements shown in Fig. 8d, 8e, 8f.

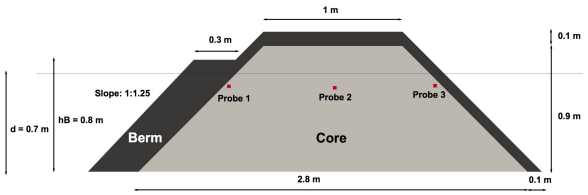

Figure 7: Berm breakwater geometry (h_B/d = 1.14)

It is observed that both the velocity and pressure measurements are more or less constant for low h_B/d ratios. As this ratio reaches the range of 0.7 - 0.8, the pressure and velocities start to drop down and the lowest values are seen around h_B/d = 1.0 - 1.2. This particular range of values indicates that the berm elevation is either on par or above the still water level (SWL). This makes complete sense as the waves are breaking as they interact with the berm (Fig. 9a and Fig. 9b)and dissipates its energy resulting in low pressures and velocities inside the breakwater. As the ratio increases further, the pressure and velocity values also increases the waves gets dissipated further inside the berm (Fig. 9c and Fig. 9d). From these plotted measurements against the corresponding berm height indicate that the optimum height would be somewhere close the SWL.

This needs to be verified with the relations in theory as well. According to the rock manual CIRIA et al., the height of the berm should be in the range of h_B = (0.5 - 0.9) Hs (m) above the design water level. In this study, the berm height h_B = 0.8 m corresponds to 0.5 times the significant wave height (lower range) above the SWL and h_B = 0.88 m corresponds to 0.9 times the significant wave height Hs (higher range) above the SWL (Table 2). According to van der Meer (2014) van der Meer and Sigurdarson (2014), the first and easiest criterion

is that the berm level should be at least 0.6 H_S above the design water level. This is the situation where the h_B/d ratio is between 1.14 and 1.21 and it can be seen from Fig. 8 that the velocities and pressure are the lowest for those h_B/d values. The simulated case for a h_B/d ratio of 1.14 is shown in Fig. 10. As the wave crest approaches the front slope of the berm breakwater, the crest shoals and breaks on the top of the berm of the breakwaters and thereby dissipating a large part if the wave energy.

Table 2: Berm height according to Rock Manual CIRIA et al.

d_B	**0.5** H_S	**0.6** H_S	**0.7** H_S	**0.8** H_S	**0.9** H_S
h_B	0.80	0.82	0.84	0.86	0.88
h_B/d	1.14	1.17	1.2	1.23	1.25

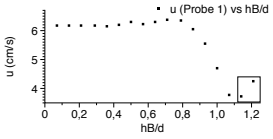

(a) Probe 1 - Velocity

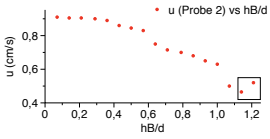

(b) Probe 2 - Velocity

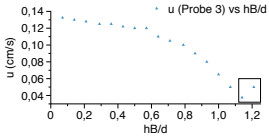

(c) Probe 3 - Velocity

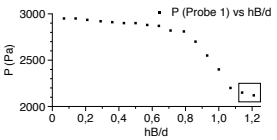

(d) Probe 1 - Pressure

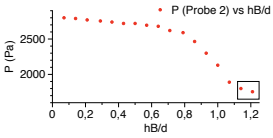

(e) Probe 2 - Pressure

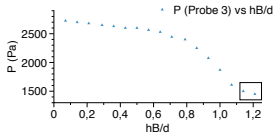

(f) Probe 3 - Pressure

Figure 8: Velocity and pore pressure variation inside berm breakwater with different berm height, boxes indicating theoretical range

Berm width vs. Velocity and pressure

The berm width (W) for berm breakwaters are normally governed by balancing breakwater cost and the expected recession if the berm is expected to reshape. The later primarily depends on the expected structural behaviour under design waves, that is if they are hardly, partly or fully reshaping. The resiliency of the berm breakwater decreases with increasing stability number. Since the berm of the breakwater simulated has a lower stability number, it is expected to be more stable without any major reshaping of the berm. In general, the

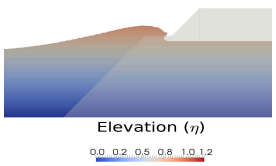

(a) h_B/d =1.07

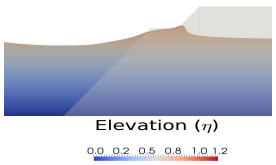

(b) h_B/d =1.14

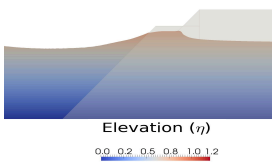

(c) h_B/d =1.21

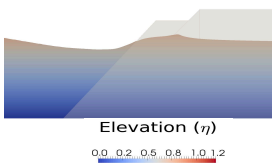

(d) h_B/d =1.28

Figure 9: Free surface near berm for different h_B/d ratio

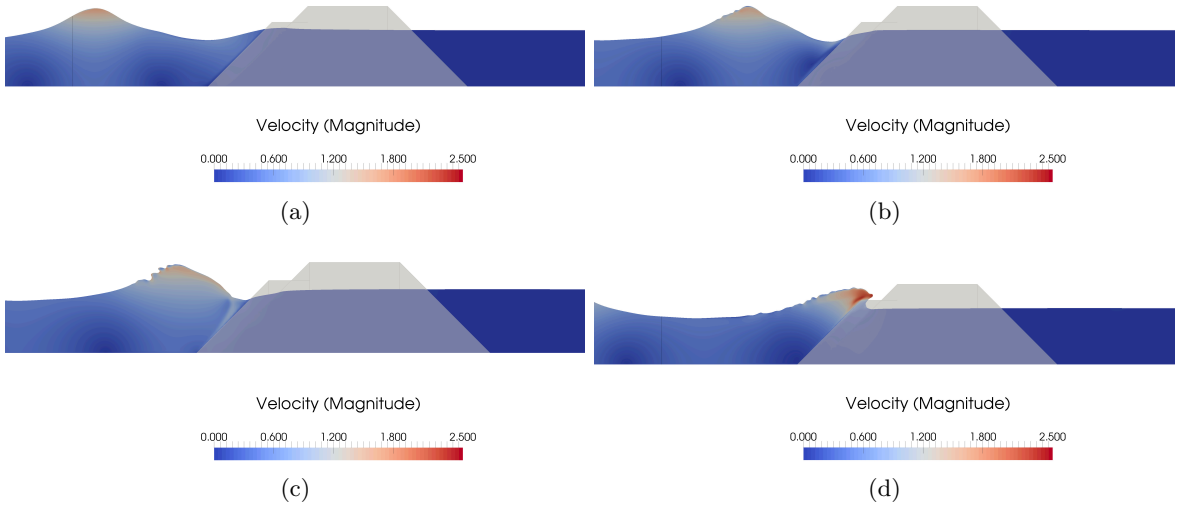

Figure 10: Free surface near berm for h_B/d ratio of 1.14

minimum berm width should be the expected recession from design waves, for example the 1:1000 year wave. van der Meer (2014) van der Meer and Sigurdarson (2014) proposed the following criteria relating the expected recession R_{ec} and required berm width B (Table 3).

Table 3: Berm width for acceptable recession van der Meer and Sigurdarson (2014)

Type	**Reshaping characteristics**	**P%**	R_{ec}/D_{n50}
Very Resilient	Hardly reshaping	10 - 20 %	0.5 - 2
Good Resiliency	Partly reshaping	20 - 40 %	1 - 5
Minimum Resiliency	Fully reshaping	<= 70 %	3 - 10

Here the resiliency is given as P %, which indicates P % of the berm width may be eroded under design wave conditions. For a fully reshaping berm, the P % can go up to 100 %. A lower limit for P % is always the safest option, but will result in a costlier berm. The berm width based the resiliency is given by 14.

$$\begin{aligned} B &= R_{ec}/(P\%/100) \\ B_{min} &= R_{ec} + 1D_{n50} \end{aligned} \tag{14}$$

For the study on the berm width, simulation are done with varying berm width (W) from 0.05 to 1.5. The berm height is kept at h_B=0.8 m, the water depth at d=0.7 m and the slope at 1:1.25. The measured velocity and pressure from the three probes are shown in Fig. 11. From Eq. 14, with R_{ec}=1.25 D_{n50} and P = 10%, this results in a berm width of 0.88 m ($w/d = 1.25$) and with P = 20%, gives a berm width of 0.44 m ($w/d = 0.63$) . It is observed

from Fig. 11, the pressure and velocity values corresponding to these w/d range are the lowest and there is no significant decrease with the increase in w/d values. The design berm width then should be in between this range of w/d ratio which satisfies the cost criterion.

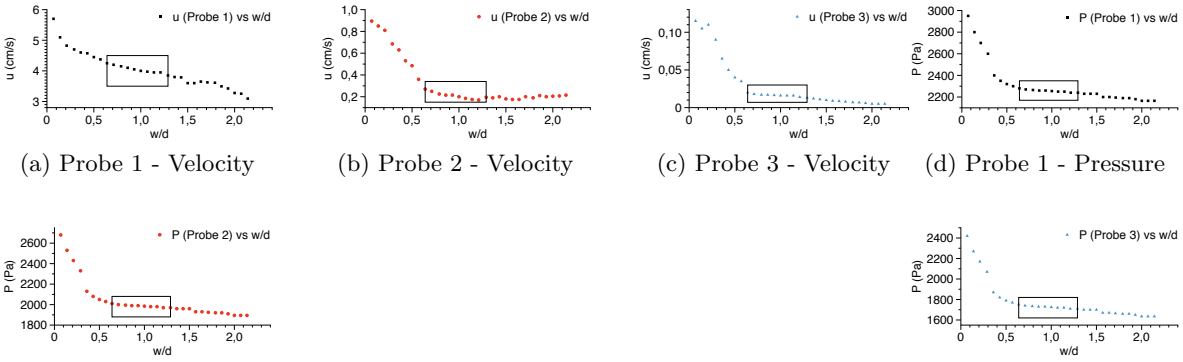

(a) Probe 1 - Velocity (b) Probe 2 - Velocity (c) Probe 3 - Velocity (d) Probe 1 - Pressure

(e) Probe 2 - Pressure (f) Probe 3 - Pressure

Figure 11: Velocity and pore pressure variation inside berm breakwater with different berm width, boxes indicating theoretical range

Berm slope vs. Velocity and pressure

Conventional berm breakwaters are not usually designed for slope angles steeper than 1:1.3. It is difficult in practice to design steeper slope angles because they become too unstable and need very large rocks. The use of concrete units with slope angles of 1:1.3 can be constructed, as concrete units will possibly have additional stability from interlocking than from weight alone. In practice for berm breakwaters, a 1:1.5 slope is actually the most gentle slope considered van der Meer and Sigurdarson (2017). In some scenarios slopes of 1:1.25 or 1:1.1 are built, which are close to the natural angle of repose of the rock and these slopes are not very stable. In some cases, like for the fully reshaping berm breakwater, this is not a problem as large reshaping is expected. For hardly reshaping structures, however, a slope steeper than 1:1.5 will increase damage as well as recession. This will result in the need for larger stones and hence is more costly to construct.

In order to study the influence of slope angle on the pore pressure and velocities inside the breakwater, simulations are done with varying slope from 1:1, to 1:1.35. The berm height is set at h_B=0.8 m, water depth d=0.7 m and berm width W=0.45 m. The measured velocity and pressures are shown in Fig. 12, and it can be seen that as the slope becomes more steeper, the velocity and pressure increases.

CONCLUSIONS

The aim of this study was to introduce the numerical modelling tool for designing berm breakwaters. The study is conducted using the numerical model REEF3D which uses the VRANS equations to solve the porous flow. The numerical model was first validated for a 2D dam break case where experimental and numerical results are compared. Comparisons for free surface show a good match and also the flow regimes of porous media flow have been

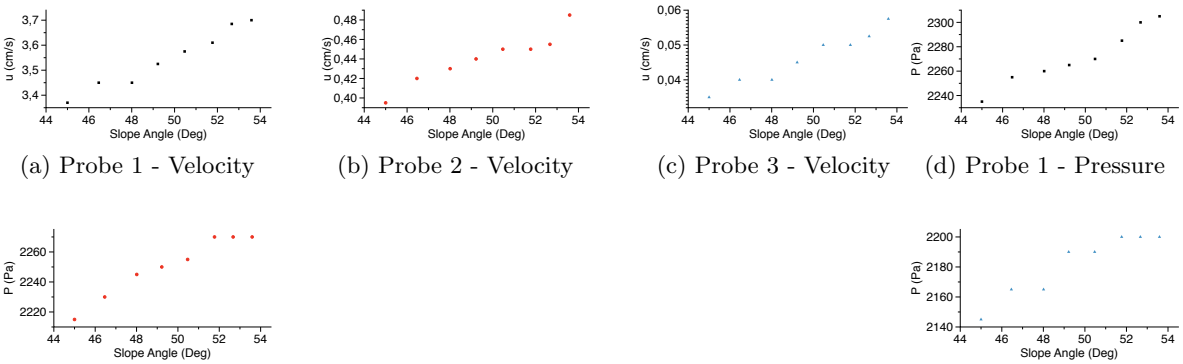

(a) Probe 1 - Velocity (b) Probe 2 - Velocity (c) Probe 3 - Velocity (d) Probe 1 - Pressure

(e) Probe 2 - Pressure (f) Probe 3 - Pressure

Figure 12: Velocity and pore pressure variation inside berm breakwater with different berm slope

correctly modelled, demonstrating the model capabilities. The study on berm breakwaters was conducted next. From the designers point of view it is important to design a berm breakwater which fulfils all the required conditions for the stability along with it being cost effective. The berm is the most important section of a berm breakwater where an optimal design can reduce the required quantity and size of rocks. The numerical model REEF3D is applied to show how to extend the database obtained with purely numerical results, simulating different structural alternatives for the berm. Different simulations are conducted with varying berm geometry. The influence of the berm geometry on the pore pressure and velocities is studied. For the berm height it is seen that the lowest values of pressure and velocities inside the core are seen when the berm height is 1.0 - 1.2 times the water depth. The width of the berm is influenced by the amount of recession that is acceptable. In this study, a statically stable berm is modelled , a very low recession is expected (P = 10-20%). It is seen that in order to obtain the required resiliency, a w/d of 0.63 is required, which will have lower values for pore pressure and velocities inside the berm. Similarly, it is seen that as the slope becomes steeper the pressure and velocities inside the core also increases. Concluding, the advanced numerical modelling of wave and coastal Structures interaction helps in designing breakwaters and offers interesting research opportunities. It is recommended that the combined use of physical models and numerical models can lead to different forms of improvements, mainly in increasing the quality at the same cost or obtaining the same quality at reduced cost. It is recommended to do further research using numerical models on berm breakwaters with different wave and material characteristics. The effect of wave height, wave period, D_{n50} and porosity on the wave kinematics insides the breakwater should be studied.

ACKNOWLEDGEMENTS

This research was supported in part with computational resources at NTNU provided by The Norwegian Metacenter for Computational Sciences (NOTUR), http://www.notur.no.

References

Berthelsen, P.A. and Faltinsen, O.M. (2008). A local directional ghost cell approach for incompressible viscous flow problems with irregular boundaries. *Journal of Computational Physics*, **227**, 4354–4397.

Bihs, H. and Kamath, A. (2016). A combined level set/ghost cell immersed boundary representation for floating body simulations. *International Journal for Numerical Methods in Fluids*. ISSN 1097-0363.

Bihs, H., Kamath, A., Arntsen, Ø.A., Chella, M. and Aggarwal, A. (2016). A new level set numerical wave tank with improved density interpolation for complex wave hydrodynamics. *Computers Fluids*, **140**, 191–208.

CECW-EH (????). *Coastal Engineering Manual, EM 1110-2-1100, part V and VI.* US Army Corps of Engineers. Washington, DC (USA).

Center for Applied Scientific Computing (2006). *HYPRE high performance preconditioners - User's Manual*. Lawrence Livermore National Laboratory.

Chorin, A. (1968). Numerical solution of the Navier-Stokes equations. *Mathematics of Computation*, **22**, 745–762.

CIRIA, CUR and CETMEF (????). *The Rock Manual. The use of rock in hydraulic engineering (2nd edition). ISBN 978-0-86017-683-1.* C863, CIRIA, London (UK).

Grotle, E.L., Bihs, H., Pedersen, E. and Æsøy, V. (2016). Cfd simulations of non-linear sloshing in a rotating rectangular tank using the level set method. *ASME. International Conference on Offshore Mechanics and Arctic Engineering*. 10.1115/1.404050810.1115/OMAE2016-54533.

Howes, F. and Whitaker, S. (1984). The spatial averaging theorem revisited. *Chemical Engineering Science*, **40**, 1387–1392. 10.1115/1.404050810.1016/0009-2509(85)80078-6.

Jacobsen, N.G., Fuhrman, D.R. and Fredsøe, J. (2012). A wave generation toolbox for the open-source CFD library: OpenFOAM. *International Journal for Numerical Methods in Fluids*, **70**(9), 1073–1088.

Jensen, B., Jacobsen, N.G. and Christensen, E.D. (2014). Investigations on the porous media equations and resistance coefficients for coastal structures. *Coastal Engineering*, **84**, 56 – 72. ISSN 0378-3839. 10.1115/1.4040508https://doi.org/10.1016/j.coastaleng.2013.11.004.

Jiang, G.S. and Shu, C.W. (1996). Efficient implementation of weighted ENO schemes. *Journal of Computational Physics*, **126**, 202–228.

Kamath, A., Alagan Chella, M., Bihs, H. and Arntsen, Ø.A. (2016). Breaking wave interaction with a vertical cylinder and the effect of breaker location. *Ocean Engineering*, **128**, 105 – 115.

Liu, P., Lin, P., Chang, K. and Sakakiyama, T. (1999). Numerical modeling of wave interaction with porous structures. *J. Waterw. Port Coast. Ocean Eng.*, **125**, 322–330.

Osher, S. and Sethian, J.A. (1988). Fronts propagating with curvature- dependent speed: algorithms based on Hamilton-Jacobi formulations. *Journal of Computational Physics*, **79**, 12–49.

Peng, D., Merriman, B., Osher, S., Zhao, H. and Kang, M. (1999). A PDE-based fast local level set method. *Journal of Computational Physics*, **155**, 410–438.

PIANC (2003). *State-of-the-Art of Designing and Constructing Berm Breakwaters.* WG40.

Troch, P. (2000). Experimentele studie en numerieke modellering van golfinteractie met stortsteengolfbrekers. *Ph.D. thesis. Faculty of Engineering and Architecture, Ghent University, Ghent (Belgium)*, 131–160.

van der Meer, J. (1998). Rock slopes and gravel beaches under wave attack. *Doctoral thesis, Delft University of Technology, Delft (The Netherlands).*

van der Meer, J. and Sigurdarson, S. (2013). Front slope stability of the icelandic-type berm breakwater. *Coastal Structures 2011.*

van der Meer, J. and Sigurdarson, S. (2014). Geometrical design of berm breakwaters. *Coastal Engineering Proceedings*, **1**(34), 25.

van der Meer, J. and Sigurdarson, S. (2017). *Design and construction of berm breakwaters.* World Scientific Publishing Co. Pte. Ltd., 5 Toh Tuck Link, Singapore - 596224.

van Gent, M. (1992*a*). Formulae to describe porous flow. *Communications on hydraulic and geotechnical engineering, Delft University of Technology, Delft (The Netherlands)*, **92-2**, 42–46.

van Gent, M. (1992*b*). Stationary and oscillatory flow through coarse porous media. *Communications on hydraulic and geotechnical engineering,Delft University of Technology, Delft (The Netherlands)*, **93-9**, 42–46.

Wilcox, D.C. (1994). *Turbulence modeling for CFD.* DCW Industries Inc., La Canada, California.